Int. J. Multiphase Flow Vol. 9, No. 5, pp. 511–530, 1983
Printed in Great Britain.

0301-9322/83 $3.00 + 00
Pergamon/Elsevier

SEPARATED TWO-PHASE FLOW MODEL: APPLICATION TO CRITICAL TWO-PHASE FLOW

H. J. RICHTER
Dartmouth College, Thayer School of Engineering, Hanover, NH 03755, U.S.A.

(*Received* 12 *October* 1981; *in revised form* 13 *March* 1983)

Abstract—A separated flow model has been developed to allow the calculation of critical flow rates for steam-water mixtures. This model considers hydrodynamic as well as thermal non-equilibrium effects which are present due to rapid depressurization. Thus, this model incorporates interphase interaction terms for momentum, energy and mass. The mass transfer, evaporation or condensation rate, is coupled with the heat transfer between the two phases. Certain empiricisms are necessary to be included into this model, e.g. the size and number of nucleation sites at the onset of flashing. Transitions from one flow regime to the other are assumed to occur at certain void fractions. Justification of these assumptions is only possible by comparison with experimental results of different authors which in general shows good agreement.

1. INTRODUCTION

The concern about light water reactor safety has resulted in considerable research efforts in the last two decades. After a postulated break in a light water reactor cooling fluid circuit, flashing of the fluid will occur as soon as the pressure in the system falls below the saturation pressure. From that moment on a two-phase mixture of vapor and liquid will be flowing at least in parts of the circuit. Depending upon the velocity, the mass fraction of vapor and the thermodynamic properties, this mixture can move in very different "flow regimes", e.g. bubble, slug, and annular flow regime. Neither these flow regimes nor the transition from one flow regime to the other are very well understood. In spite of that, very extensive computer codes were developed to predict *a priori* the behavior of the fluid under such emergency conditions in a reactor.

Of special concern is the mass flow rate exiting through a break in the cooling fluid circuit. This mass flow rate will define the time until the reactor core becomes uncovered, and how much water has to be pumped back in order to assure sufficient cooling. The knowledge of this maximum flow rate which can exit through such a break is essential for an accurate assessment of the overall behavior. Therefore, it was properly named the "critical" mass flow rate. This critical two-phase flow is the maximum possible mass flow rate through a given break geometry or a pipe for given upstream conditions. In general, the critical mass flux is achieved when

$$(\partial G/\partial p)_s = 0 \qquad [1]$$

with G the mass flux and p the local pressure. The subscript s indicates that the thermodynamic path is usually assumed to be isentropic. Equation [1] is sometimes called the choking criterion.

This report describes the application of a newly developed separated two-phase flow model (two-fluid model) for the problem of critical two-phase flow. The main emphasis is on the derivation of an analytical model, which includes the major relevant physical phenomena, and can be used to make predictions suitable for comparison with experimental data. Hydrodynamic as well as thermal non-equilibrium effects are considered. The evaporation or condensation rate is assumed to be limited by the heat transfer between the two phases.

2. PREVIOUS WORK

Comprehensive reviews of critical two-phase flow were performed, e.g. by Jones & Saha (1977), Saha (1978), Wallis (1980) and Isbin (1980). Only a short summary of the previous work will be mentioned here in order to highlight differences to the separated flow model developed in this report.

There are two types of non-equilibrium flow models, on the one side only velocity differences between the phases are considered (hydrodynamic non-equilibrium), while thermal equilibrium is assumed to be established. A second group of investigators assumes that the velocity ratio is close to unity, but thermal non-equilibrium is of major inportance. In addition to that, two-dimensional effects as well as diameter effects are believed by some to be the main cause of deviation between predictions and experiments. Some of the researchers include several of the effects mentioned above in their models.

2.1 *Hydrodynamic non-equilibrium models*

Considering different flow regimes of flow, it is apparent that a homogeneous two-phase flow model is not capable of describing different flow regimes. The phases have different densities and in many cases are not dispersed uniformly. Several authors have derived the velocity ratio of the two phases from first principles and found it to be only a function of the density ratio independent of the flow regime, e.g. Vance (1962), Fauske (1963), Cruver (1963) and Zivi (1964).

In contrast it is known that in bubbly flow, which usually exists for a void fraction of $\alpha < 0.2$ or 0.3 the velocity ratio is not too far from unity, e.g. Muir & Eichhorn (1967) or Kuo *et al.* (1979).

In spite of this obvious discrepancy between theory and experiment, the above choked flow models are able to predict the critical mass flux fairly well in some cases. Since the critical mass flux is not too sensitive to the velocity ratio as can be seen from figure 1. All the curves are calculated for constant entropy during change of state.

The isentropic homogeneous equilibrium model (IHE) underpredicts the critical mass flux in some cases, but is quite successful for the prediction of flow in longer pipes. On the one hand

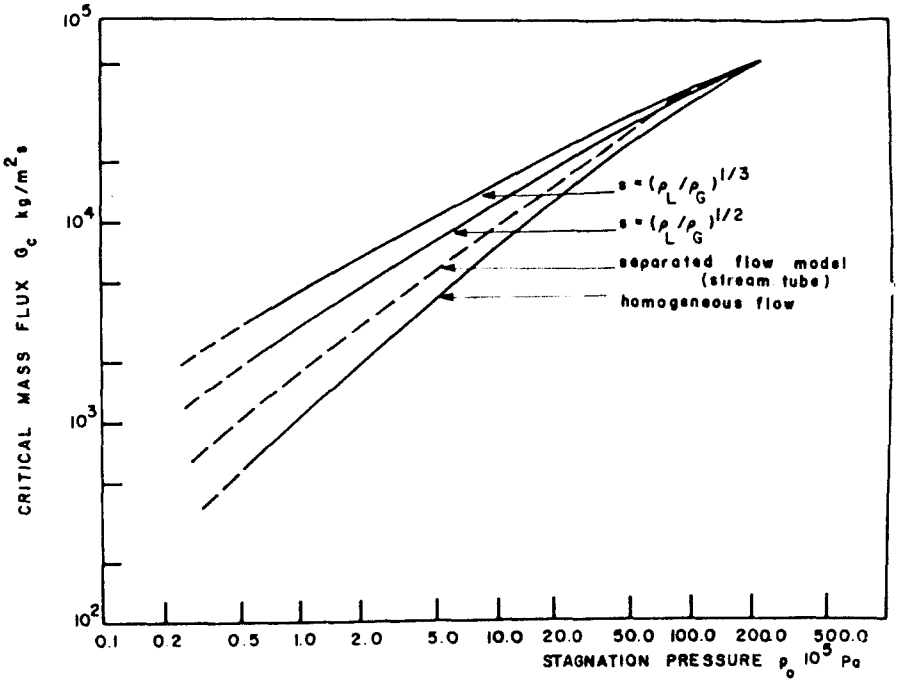

Figure 1. Critical mass flux vs stagnation pressure for saturated water at inlet.

the velocity ratio tends to increase the predicted mass flux; on the other hand friction decreases the critical mass flux. It is suspected that both contrary effects result in reasonable predictions with the homogeneous equilibrium model.

2.2 *Thermal non-equilibrium models*

Thermal non-equilibrium—temperature differences between the phases—is believed to be the major cause of deviation between predictions and experimental results, especially if subcooled fluid enters the test section or in a very short test section.

Homogeneous equilibrium flow assumes no heat transfer resistance; that means the latent heat necessary for evaporation or the latent heat set free during condensation is distributed immediately throughout the whole fluid. Actual fluids have heat resistances (e.g. at the interface), and therefore, it takes time before locally released or needed heat is transported. Especially in rapidly accelerating flows, the time to transport the heat might be in the same order of magnitude as the residence time in the flow conduit. Therefore, in expanding two-phase flow, relaxation will occur and consequently departure from thermodynamic equilibrium prevails.

The extreme case would be frozen flow, where no quality change is assumed, Henry & Fauske (1971). In this case, only the already existing vapor would expand. Except for some flow experiments through orifices, this theory overestimates the flow rate considerably as indicated by Ardron & Furness (1976), while the equilibrium model underestimates the mass flux in most cases. Hence, in the actual case it may be expected that partial evaporation takes place, even when the flow path is relatively short.

Henry (1970b) and Henry & Fauske (1971) tried to cope with thermal non-equilibrium by introducing an empirical coefficient, which represents the deviation from the homogeneous equilibrium model. It is directly proportional to the difference between the exit quality. The model does not try to represent the physical events.

Shrock *et al.* (1977) developed a two step model. Initially "frozen" flow was assumed (constant quality) until the pressure dropped by a certain amount below the saturation pressure, at which point sudden equilibrium was achieved and downstream from this point frozen flow occurred again. It is appreciated by the authors that the model does not represent the real physical behavior but they claim there is no satisfactory means to predict the number and size of microbubbles in the liquid triggering the nucleation process.

A similar approach was accomplished by Edwards (1968). He assumed an arbitrary delay time before flashing starts as a function of the subcooling in the reservoir. Therefore, at the onset of flashing the liquid is already superheated. Furtheron he assumed that the bubble growth is limited by heat conduction to the interface using the analysis of Plesset & Zwick (1954). In addition, Edwards assumed that there are about 10^{12} to $10^{13}\,m^{-3}$ nucleation sites present at the onset of flashing.

Bailey (1951) preheated the water to reduce the amount of dissolved air and found an increase in mass flux. This indicates that dissolved gases are important in consideration of non-equilibrium aspects.

2.3 *Separated flow models*

In this approach, usually separate conservation equations are developed for each phase, Bouré (1974), Ishii (1975). Therefore, these equations have to contain terms describing heat, mass and momentum transfer between the phases. These transport equations are normally not very well known, thus simplifications of the above equations or arbitrary assumptions are introduced to overcome the lack of knowledge. The advantage of the separated flow model is its capability to deal not only with hydrodynamic non-equilibrium between the phases but also with their temperature differences.

Wolfert (1976) assumed a constant relative velocity of 0.15 m/s a bubble population of

number $5 \cdot 10^9\,m^{-3}$ and a minimum void fraction of 10^{-6}, thus the minimum bubble diameter is $7.2 \cdot 10^{-6}$ m.

Rohatgi & Reshotko (1975) assumed essentially an isothermal flow of the liquid and bubble growth limitation due to heat conduction. About $10^6\,m^{-3}$ heterogeneous nucleation sites were selected, only comparisons with nitrogen experiments were performed. Malnes (1975) looked in more detail into the question of nucleation sites. He claims that the release of dissolved gas is the main mechanism for bubble formation during decompression. He could explain the data by Henry (1968, 1970) only if he assumed in his model bubble growth controlled by heat conduction and a velocity ratio close to unity. Furtheron, he had to suppose a gas content of $4 \cdot 10^{-2}\,m^3/m^3$ at 25°C and 10^5 Pa. Zaloudek's (1964) experiments could only be matched by assuming a gas content of $5 \cdot 10^{-4}\,m^3/m^3$ at the same conditions, thus the gas content is two orders of magnitude lower in the latter case.

Rivard & Travis (1980) chose an initial number of bubbles of $10^9\,m^{-3}$ as well as an initial void fraction of $2 \cdot 10^{-4}$ which results in an initial bubble diameter of $7.2 \cdot 10^{-5}$ m.

In all these separated flow models there was an attempt to simplify the set of equations by introducing an empirical equation for the velocity ratio.

Ardon *et al.* (1976, 1978) wrote different equations for both phases and described the interfacial forces in the bubble flow regime as the sum of drag and virtual mass force. They suggest that the heat transfer from the liquid to the bubble takes place mainly by diffusion, thus no convection term is included. Yet in a later paper, Ardron and Ackerman (1978) concluded from experiments that the convection model of heat transfer is dominant. In their model, changes in liquid temperature were not accounted for. The analysis is therefore limited to very small steam fractions. In addition, it is assumed that the liquid superheat must exceed some critical value before appreciable nucleation takes place. This superheat was taken to be $\Delta T = 3$°C. They also introduced a rate equation for the formation of bubble nuclei. The effective initial density of heterogeneous nucleation sites was assumed to be $10^6\,m^{-3}$. Additionally, the vapor is taken to be an ideal gas, therefore the pressure range where this model is applicable is limited. Lyczkowski & Solbrig (1977) evaluated a separated flow model for unsteady state. A mass transfer rate as a function of relaxation time and empirical threshold quality is developed. Unfortunately, only comparison with one experiment is shown.

All the models described in this chapter account for thermal nonequilibrium between the phases during flashing. The models are usually restricted to bubbly flow and either the limited heat conduction or convection is made responsible for the deviation from thermodynamic equilibrium. Some attempts are made to account for unequal velocities between the phases either by empirical correlations or by introducing interfacial voice terms, (Ardron *et al.* 1978).

3. THIS SEPARATED FLOW MODEL

From the preceding literature review, it is apparent that all critical flow models have certain deficiencies which seem to prevent general application. Some models were developed simply by correlating data and finding an empirical relationship. In other models, thermal and/or hydrodynamic non-equilibrium are considered, but these models are mainly limited to the bubbly flow regime. There are many uncertainties in critical mass flow, such as the effect of geometry, e.g. Simon (1972), two-dimensional flow effects and even the location where the choking occurs seems to be in question, e.g. Henry (1968). Therefore, one cannot expect to overcome all empiricism in this complex flow easily where heat, mass and momentum transfer are present simultaneously. Nevertheless, it is believed that improvements are possible by developing a set of separated conversation equations for each phase and transfer equations to describe the flow behavior of flashing two-phase flow (Richter and Minas 1979, Richter 1981).

It was shown by Kuo *et al.* (1979) that an appreciable improvement of the bubble flow regime is possible if separated conversation equations of mass and momentum are solved. This requires the knowledge of the interfacial terms—like the interfacial forces—in the momentum

equation. But during flashing, the mass transfer has to be described also, in order to predict the overall behavior of the flow and especially the critical two-phase flow. Information about heat, mass and momentum transfer is not only needed for the bubbly flow regime, but for other regimes also.

In the model developed here, separated flow was considered with the following assumptions:

(a) Steady-state flow.

(b) Liquid and vapor can have different velocities. These will be evaluated by appropriate interfacial forces.

(c) Mass transfer is limited by heat transfer between the phases. Heat transfer coefficients will include conduction as well as convection, as appropriate.

(d) Friction pressure drop is included—this is especially important for blowdown through long pipes.

(e) The flow is considered to be one-dimensional. There is some discussion about two-dimensional effects, but these are uncertain and thus this increased complexity has been avoided.

3.1 *Mass conservation equation*

The conservation equations for mass for both phases are (Wallis 1969): For the liquid (phase L),

$$\frac{1}{W_L}\frac{dW_L}{dz} = \frac{1}{\rho_L}\frac{d\rho_L}{dz} + \frac{1}{v_L}\frac{dv_L}{dz} - \frac{1}{1-\alpha}\frac{d\alpha}{dz} + \frac{1}{A}\frac{dA}{dz} \qquad [2]$$

where W is the mass flow rate, ρ the density, v the velocity, α the void fraction, A the total cross section and z the coordinate in the flow direction.

For vapor (phase G),

$$\frac{1}{W_G}\frac{dW_G}{dz} = \frac{1}{\rho_G}\frac{d\rho_G}{dz} + \frac{1}{v_G}\frac{dv_G}{dz} + \frac{1}{\alpha}\frac{d\alpha}{dz} + \frac{1}{A}\frac{dA}{dz} \qquad [3]$$

dW_G/dz is the evaporation rate, thus we can write:

$$dW_G/dz = -dW_L/dz = W(dx/dz) \qquad [4]$$

with W the total steady-state flow rate and x the vapor mass fraction.

The compressibility of the liquid is included and the vapor is treated as a real gas. In many cases the compressibility of the liquid

$$\frac{d\rho_L}{dz} = \left(\frac{\partial\rho_L}{\partial p}\right)_{sat}\frac{dp}{dz}$$

can be neglected, but at high pressures close to the critical points, this compressibility might be of importance, e.g. for water at 15 MPa (2200 psia) at saturation we have

$$\frac{(\partial\rho_L/\partial p)_{sat}}{(\partial\rho_G/\partial p)_{sat}} = -1.7. \qquad [5]$$

Even more important is the real gas effect. At a pressure of 1 MPa the compressibility factor for saturated vapor is $Z = p/\rho RT = 0.93$ and for pressure of 10 MPa, $Z = 0.67$. The real gas effect increases the predictions of critical mass flux somewhat. As an example, Sozzi &

Sutherland (1975) measured for an upstream pressure $p_0 = 6.2$ MPa and a quality of $x_0 = 0.0008$, a critical mass flux of 31,200 kg/m^{2}s in a 0.11 m pipe with a diameter of 12.7 mm. This separated flow model including the real gas effect predicts a critical mass flux of 29,700 kg/m^{2}s (about 5% too low) while the model calculates a mass flux of 28,100 kg/m^{2}s (about 10% too low) if the vapor is treated like an ideal gas ($Z = 1$). With increase in pressure, the differences between these two predictions will increase.

3.2 *Momentum conservation equations*

The conservation equations for momentum for the two phase are written in the following way using [4] for the liquid phase:

$$\rho_L v_L (1-\alpha) A \frac{dv_L}{dz} = -\frac{dp}{dz}(1-\alpha)A + F_{LG}A - F_{wL}A - (1-\eta)(v_G - v_L)W\frac{dx}{dz} - \rho_L g(1-\alpha)A\cos\theta \quad [6]$$

where θ is the inclination angle of the flow conduit to the vertical.

For the vapor phase,

$$\rho_G v_G \alpha A \frac{dv_G}{dz} = -\frac{dp}{dz}\alpha A - F_{LG}A - F_{wG}A - \eta(v_G - v_L)W\frac{dx}{dz} - \rho_G g\alpha A\cos\theta \quad [7]$$

F_{LG} is the interfacial momentum transfer per unit volume. The terms F_{wL} and F_{wG} are the average interfacial forces per unit volume between either phase and the wall. Except in the droplet flow regime, the vapor phase has almost no contact with the wall therefore we might write as well,

$$F_{wG} \simeq 0$$

and thus only F_{wL} accounts for the wall friction, which is introduced from Martinelli & Nelson (1948) to be

$$F_{wL} = \phi_{f0}^2 \left(\frac{dp}{dz}\right)_{F_{f0}} \quad [8]$$

where $(dp/dz)_{F_{f0}}$ is the friction pressure drop assuming the total flow rate to be liquid and ϕ_{f0}^2 is an empirical two-phase multiplier introduced by Martinelli and Nelson, which is a function of equilibrium quality x and the pressure.

The second to last term in the two momentum equations [6] and [7] evaluates the momentum exchange due to mass transport (evaporation or condensation). When liquid is evaporating, its velocity is changing from v_L to v_G, the force associated with this velocity change is described with this term. The coefficient is not well known. Wallis (1969) has shown that for a reversible flow the coefficient η should be

$$\eta = 0.5.$$

This author studied the influence of the coefficient η on the predictions of pressure drop by varying η between $0 \le \eta \le 1$ and found only minor influences indicating that the effect of this term is small. With $\eta = 1$, the total force is charged to the vapor, the pressure drop is slightly lower than with $\eta = 0$, but choking was usually predicted at approximately the same mass flow rate. The interfacial force F_{LG} is known quite well for bubbly as well as for annular flow. In the

bubbly flow regime this force is:

$$F_{LG} = \frac{3}{4}\frac{(C_D)1-\alpha}{d}\alpha(1-\alpha)^3\rho_L(v_G - v_L)|v_G - v_L| + C\rho_L v_G\alpha\, d/dz(v_G - v_L). \quad [9]$$

The first term on the r.h.s. represents the drag force, the second term the apparent mass force due to the change in kinetic energy induced by the bubble motion in the liquid. For a sphere, the constant C is 0.5 which was used in this model.

With the volumetric flux j_{L0} given by

$$j_{L0} = (v_G - v_L)(1-\alpha) \quad [10]$$

and a bubble Reynolds number

$$\mathrm{Re} = \frac{\rho_L j_{L0} d}{\mu_L} \quad [11]$$

where d is the diameter of the bubble, we obtain the drag coefficient for one bubble (Wallis 1969):

$$C_D = \frac{24}{\mathrm{Re}}(1 + 0.15\,\mathrm{Re}^{0.687}) \quad [12]$$

and for $\mathrm{Re} > 1000$ we have

$$C_D = 0.44. \quad [13]$$

These correlations were originally developed for spherical particles in a fluid, but the drag coefficient should be valid for bubbles as well especially if the bubbles are not distorted and internal circulation is negligible.

Finally, since we have many bubbles which might interfere with each other, the drag has to be a function of the bubble concentration. Rowe and Henwood (1961) suggested the correlation:

$$(C_D)_{1-\alpha} = C_D(1-\alpha)^m. \quad [14]$$

The exponent $m = -4.7$ is almost independent of the Reynolds number, (Wallis 1969).

The momentum equations [6] and [7] are valid for all flow regimes, but the interfacial force in [9] is restricted to the bubble flow regime. If the void fraction exceeds about $\alpha_b = 0.2$ to 0.3 we can expect a transition from bubbly to another flow regime, at which bubble coalescence will occur. Further increase in void fraction will eventually lead to annular flow. Little is known about the flow regimes between bubbly and annular flow. Thus, some arbitrary assumptions about interfacial forces, heat transfer and interfacial area have to be made for these intermediate flow regimes. These assumptions can only be justified if they predict the experimental flow behavior accurately.

We approach the evaluation of the interfacial forces in the following way. We assumed that from a certain void fraction α_a on, e.g. $\alpha_a = 0.8$ the flow regime will be annular. For this flow regime the interfacial force is (Wallis 1969):

$$F_{LG} = 3\frac{C_{fi}}{D}\sqrt{(\alpha)}\rho_G(v_G - v_L)|v_G - v_L| \quad [15]$$

where C_{fi} is an interfacial friction coefficient.

$$C_{fi} = 0.005\{1 + 75(1 - \alpha)\}. \quad [16]$$

As a first approximation it was assumed that in the flow regime between bubbly and annular flow, the interfacial friction factor can be interpolated linearly with void fraction α. Therefore, for this flow regime, which will be called "churn-turbulent", the following relationship for the interfacial friction factor applies

$$C_{fi} = C_{fib} = \frac{C_{fib} - C_{fia}}{(\alpha_b - \alpha_a)}(\alpha - \alpha_b) \quad [17]$$

where α_b is the void fraction, where coalescence of bubbles starts and C_{fib} is the interfacial friction factor at this particular void fraction derived by equivalence of [9] with [15], C_{fia} is the interfacial friction factor at the onset of annular flow, to be specific, at the void fraction α_a, e.g. $\alpha_a = 0.8$ and [16]. We have varied the void fraction for onset of churn-turbulent flow from $\alpha_b = 0.2$ to 0.3 and found only significant differences in critical flow, if this transition occurs far upstream from the choking point. The equations above represent a complete description of the one-dimensional force balance for bubbly, churn-turbulent, and annular flow regime.

3.3 *Energy conservation equation*

For an adiabatic two-phase system the energy equation is:

$$\frac{dx}{dz} W[(h_G - h_L) + \tfrac{1}{2}(v_G^2 - v_L^2)] + W_G\left[\frac{dh_G}{dz} + v_G \frac{dv_G}{dz}\right] + W_L\left[\frac{dh_L}{dz} + v_L \frac{dv_L}{dz}\right] + Wg \cos\theta = 0. \quad [18]$$

If we assume that the evaporation or condensation takes place only at the interface between the two phases, we have to evaluate the interfacial area as well as the heat transfer coefficient at this interface. The latent heat has to be transported towards the interface by conduction and/or convection during evaporation, or has to be removed during condensation. In the bubbly flow regime it is relatively easy to evaluate the interfacial area if the number of bubbles per unit volume N and the average diameter of the bubbles d are known. In this case the void fraction is:

$$\alpha = N \cdot \frac{\pi d^3}{6}. \quad [19]$$

Thus the surface area per unit volume is:

$$a = N\pi d^2. \quad [20]$$

Usually there is less evaporation than equilibrium requires, since the latent heat has to be transported from the liquid core to the interface. We can therefore write:

$$\frac{6h}{d}(T_L - T_G)\alpha A = W\frac{dx}{dz} h_{LG} + W_G \frac{dh_G}{dz}. \quad [21]$$

The l.h.s. represents the rate of heat transfer due to conduction and convection to the surface, where h is the heat transfer coefficient. The first term on the r.h.s. is the energy necessary to evaporate a certain mass fraction dx over a length dz. The last term represents the change of enthalpy of the bubble due to temperature and pressure changes. We assume the vapor has always saturation temperature.

$$T_G = T_{sat} \tag{22}$$

and therefore,

$$\frac{dh_G}{dz} = \left(\frac{\partial h_G}{\partial p}\right)_{sat} \cdot \frac{dp}{dz}. \tag{23}$$

Since the conductivity of the vapor is much lower than that of the liquid, this assumption holds only for small vapor entities. Certainly in annular flow this is questionable.

The heat transfer coefficient h,[21], is described in the same way as for a flow around a single sphere.

$$Nu = \frac{hd}{k_L} = 2 + 0.6\,\mathrm{Re}_b^{1/2}\mathrm{Pr}_L^{1/3}. \tag{24}$$

The first term on the r.h.s. represents the heat conductivity term, while the second term is the contribution of convection to the overall heat transfer. Ardron (1978) observed in his critical flow experiments that the convection is the dominant mode of heat transfer. The Reynolds number in [24] has to be calculated with the relative velocities between the two phases. It differs from the Reynolds number presented in [11]:

$$\mathrm{Re}_b = \frac{\mathrm{Re}}{1-\alpha}. \tag{25}$$

Equation [24] represents the heat transfer coefficient around a single bubble or sphere. For a certain bubble population interference between bubbles is possible. This will probably result in a larger overall heat transfer. Since no correction factor has a function of bubble concentration could be found from the literature, the actual heat transfer might be underestimated.

For the newly introduced churn-turbulent flow regime it is necessary to evaluate an appropriate interfacial area and heat transfer coefficient. We will consider this particular flow regime again as a transitional regime between bubbly and annular flow.

To get the interfacial area we interpolate in a very similar fashion as for the interfacial friction factor. For the bubbly flow regime we have from [24] at onset of coalescence:

$$a_b = N \cdot \pi d_b^2 = \frac{6\alpha_b}{d_b} \tag{26}$$

where d_b is the average bubble diameter at this particular point. At the onset of annular flow at a void fraction α_a the interfacial area per unit volume is approximately

$$a_a = \frac{4\alpha_a^{1/2}}{D} \tag{27}$$

with D the hydraulic diameter of the flow conduit. thus the interfacial area per unit volume in the churn-turbulent flow is similar to [17]:

$$a = a_b + \frac{a_b - a_a}{\alpha_b - \alpha_a}(\alpha - \alpha_b). \tag{28}$$

The actual interfacial area in a certain conduit length dz would be:

$$A_i = a\,\frac{\pi D^2}{4}\,dz. \tag{29}$$

Finally, the interfacial heat transfer coefficient in the churn-turbulent flow regime will be defined. From momentum and heat transfer analogy, a correlation of the Colburn type should eventually resemble a heat transfer coefficient at the interface. The Colburn analogy results in

$$\frac{h}{\rho_L c_{pL}(v_G - v_L)} Pr_L^{2/3} = \frac{C_{fi}}{2}. \quad [30]$$

But there should be a smooth transition from the heat transfer coefficient evaluated in [24] at the breakdown of the bubble flow regime $(h_b)_{\alpha_b}$ and the one calculated in [30]. Thus we suggest that the actual heat transfer coefficient is:

$$h_{act} = (h_b)_{\alpha_b} \frac{h}{(h)_{\alpha_b}} \quad [31]$$

where h is the heat transfer coefficient from [30], and $(h_b)_{\alpha_b}$ from [24]. The Colburn analogy is restricted to flows without any form drag. Thus, $(h)_{\alpha_b}$ is a pseudo-heat transfer coefficient calculated from [30], at the transition point from the bubble to the churn-turbulent flow regime. This is only introduced to have a smooth transition from one flow regime to the order.

As mentioned above, some of the assumptions about the transitional churn-turbulent flow regime can only be justified by comparison with experimental results of different investigators.

4. SOLUTION OF THIS SEPARATED FLOW MODEL

A computer program has been developed based on the separated flow model outlined in section 3. It is based on an explicit method. It requires the input of the total flow geometry as a function of the axial coordinate z in the flow direction. In addition, upstream temperature and pressure or any other suitable thermodynamic properties have to be given to describe the stagnation state sufficiently.

A mass flow rate will be estimated, eventually causing choking in the exit cross section. The computer program will calculate pressure, temperatures of the phases, velocities of the phases, quality, and void fraction. If the flow entering the conduit is subcooled, the program will switch to a bubble flow regime shortly after the saturation point is surpassed. For a void fraction usually larger than $\alpha > 0.3$ a transition to the churn-turbulent flow regime will occur and for a void fraction $\alpha > 0.8$ annular flow is assumed. Choking is presumably reached when the pressure gradient becomes very large, e.g. $|dp/dz| > 10^4$ MPa/m.

It is known that a certain superheat of a liquid is necessary before evaporation will start. This is also true in the case where heterogeneous mucleation sites like dissolved gas bubbles are present in the liquid. As was pointed out earlier for water, these nucleation sites are the only locations where evaporation takes place. The assumption necessary to allow for a finite initial superheat in this computation scheme is to postulate an initial bubble diameter d_0. From the available data an initial bubble diameter may be assumed:

$$d_0 = 2.5 \cdot 10^{-5}\,\text{m}. \quad [32]$$

Reocreux (1976, 1977) measured the superheat before flashing starts. He ran experiments in the range of 0.1 MPa at the onset of flashing and found a superheat of 1 to 2°C. If we assume that equilibrium prevails between the inside and outside of the bubble before growth starts we get:

$$\Delta p = 4\sigma/d_0 \quad [33]$$

and with the Clausius Clapeyron equation the superheat can be evaluated:

$$\Delta T = \frac{v_{LG}}{s_{LG}} \frac{4\sigma}{d_0} \quad [34]$$

where v_{LG} is the difference in the specific volume, and s_{LG} the entropy difference between vapor and steam; σ is the surface tension. For the diameter given by [32] we get in the pressure range of Reocreux's experiments a superheat of

$$\Delta T = 1.3 \text{ to } 0.7°\text{C}. \qquad [35]$$

Malnes (1975) claimed that the water was already a certain amount of dissolved small gas bubbles—which serve as hetrogeneous nucleation sites, as described previously. Many other investigators assumed a certain number of nucleation sites. Fig. 2 shows the attempt to match the pressure profile in one of Reocreux's (1977) experiments by varying the nucleation site density N_i. In this case an initial number of $N_i \simeq 10^9\ \text{m}^{-3}$ seems to be appropriate. From Malnes' comparison with Zaloudek's (1964) data he concluded that the gas content is about $5 \cdot 10^{-4}\ \text{m}^3/\text{m}^3$, thus we would get with [32]

$$N_i \simeq 6 \cdot 10^{10}\ \text{m}^{-3}.$$

This shows generally good agreement with experimental results. In figure 3 the effect of nucleation site or initial bubble density is plotted versus the critical mass flux calculated for a short nozzle of Sozzi & Sutherland's test facility. For a very low number of nucleation sites, the flow should be close to frozen flow; for a very high number of bubbles the flow should be close to the homogeneous equilibrium flow model.

From this diagram and comparison with the assumptions of several other investigators like Edwards (1968) and Sozzi & Sutherland (1975), we concluded that an appropriate initial bubble number density is

$$N_i = 10^{11}\ \text{m}^{-3}. \qquad [36]$$

In this model is was assumed that no further nucleation sites are activated during flashing. This relatively high bubble density might compensate for the heat transfer coefficient which was

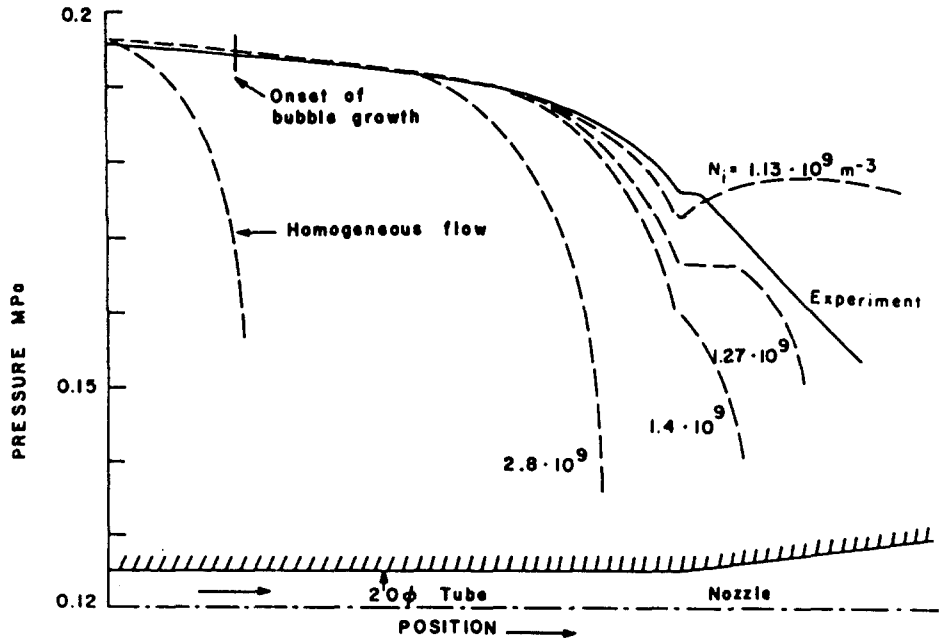

Figure 2. Pressure drop vs length of the test section. Comparison of Reocreux's (1976) experiments and different initial bubble densities.

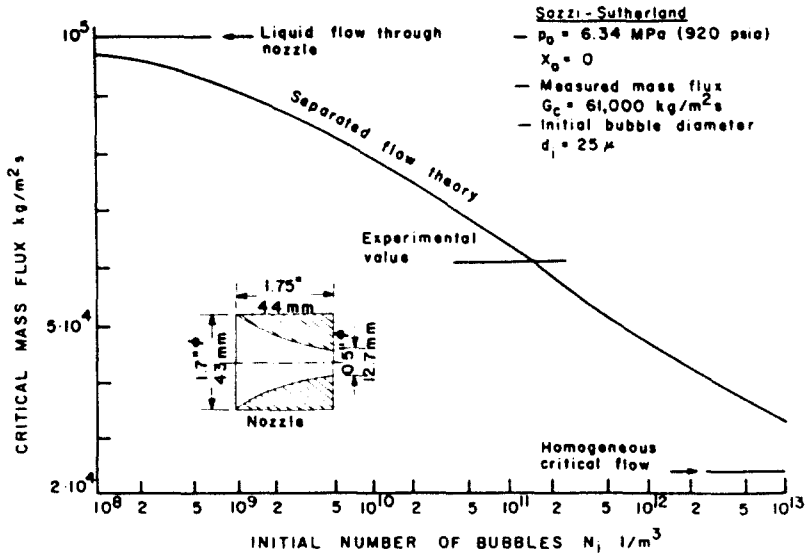

Figure 3. Effect of initial bubble density on critical mass flux. (Experiment from Sozzi & Sutherland 1975).

argued earlier to be eventually too small. Experimental verification of these assumptions are centainly needed.

5. COMPARISON OF THIS SEPARATED FLOW MODEL WITH CRITICAL TWO-PHASE FLOW EXPERIMENTS

Comparisons were made of critical flow rate predictions of this separated flow model with experimental results of different authors.

Sozzi & Sutherland (1975) performed many experiments in different nozzles and pipe lengths. For one geometry and one particular upstream conditions, the detailed results obtained from this model will be studied next.

For a stagnation pressure of $p_0 = 6.63$ MPa and an inlet quality of $x_0 = -0.0004$, these investigators measured a critical mass flux of $G_c = 33.930$ kg/m²s, while we obtained $G_c = 32.240$ kg/m²s from the calculations. Thus we underpredicted by approximately 5%. It should be mentioned that Sozzi & Sutherland present their inlet quality as

$$x_0 = \frac{v_0 - v_L(p_0)}{v_G(p_0) - v_L(p_0)}$$

where v_0 is the specific volume at inlet and $v_G(p_0)$, $v_L(p_0)$ are the specific volumina of steam and water respectively for the stagnation pressure. From these calculations were plotted the predicted pressure along the test geometry (figure 4). In the entrance nozzle a rather rapid pressure drop takes place due to the acceleration of the fluid. At the same time flashing starts. The void fraction in the nozzle is relatively small as can be seen from figure 5 and the relative velocity between the two phases seems almost negligible (figure 6). But if we look at the contribution of convection to the overall heat transfer in [24] it is already over 40% of the overall heat transfer at the end of the inlet nozzle. In spite of that, the heat transfer is too small to assure thermal equilibrium. The temperature difference between the two-phases, or the superheat of the liquid, has risen to about $\Delta T = 7$°C at the end of the nozzle (figure 7). In the pipe following the nozzle the overall pressure drop is small, but thermal non-equilibrium cannot be reestablished. About 5 cm before the end of the pipe, the void fraction increases to about $\alpha = 0.3$, so that transition to the churn-turbulent flow regime takes place according to previous assumptions. Agglomeration of bubbles will occur and with it an increase in the velocity ratio between vapor and liquid (figure 6). This allows for much higher heat transfer and thermal

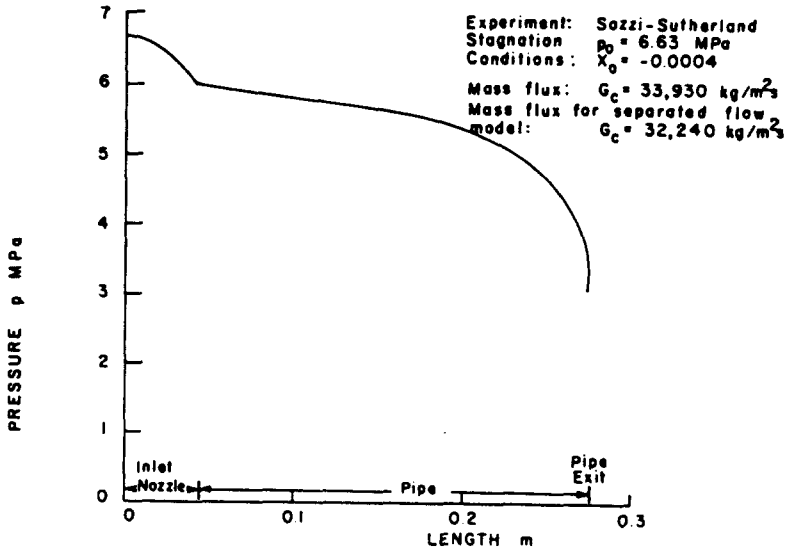

Figure 4. Pressure drop vs length of test section calculated from separated flow model. (Experiment from Sozzi & Sutherland 1975).

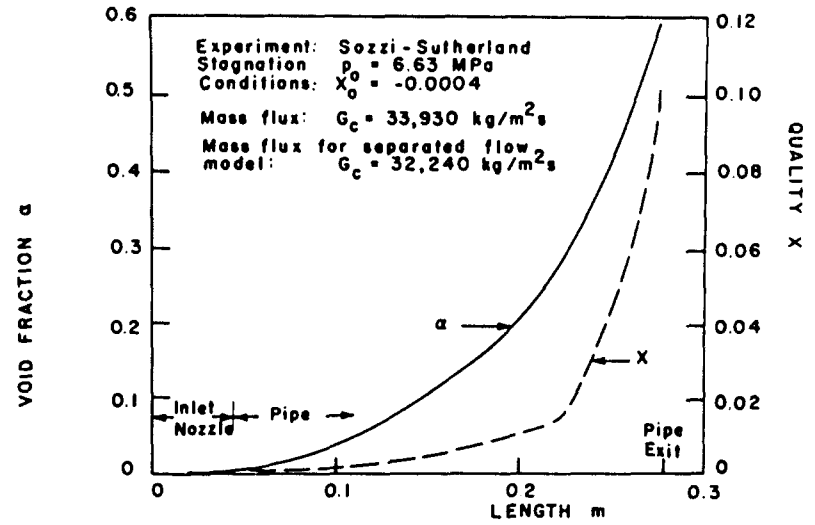

Figure 5. Void fraction and quality vs length of test section calculated from separated flow model. (Experiment from Sozzi & Sutherland 1975).

equilibrium is approached rapidly downstream from the transition, as can be seen from figure 7. At this particular point the flow is accelerating rapidly, the pressure drops sharply and choking occurs at the exit. Close to the exit, thermal nonequilibrium is increasing, as indicated by the increasing temperature difference between the phases. The exit pressure was calculated to be 3.2 MPa while Sozzi & Sutherland measured a pressure of 4.3 MPA about 0.8 mm upstream for the exit. The accuracy of exit pressure measurements was questioned by many authors, e.g. Isbin (1980), Henry (1970), Zaloudek (1965). From this one example, several interesting conclusions can be drawn:

—The velocity ratio in the bubbly flow regime is very close to unity, but nevertheless the small velocity difference between the two-phases is important for heat transfer.

—In the bubbly flow regime only thermal non-equilibrium is important.

—In the churn-turbulent flow regime, thermal equilibrium is reestablished, but hydrodynamic non-equilibrium becomes increasingly important.

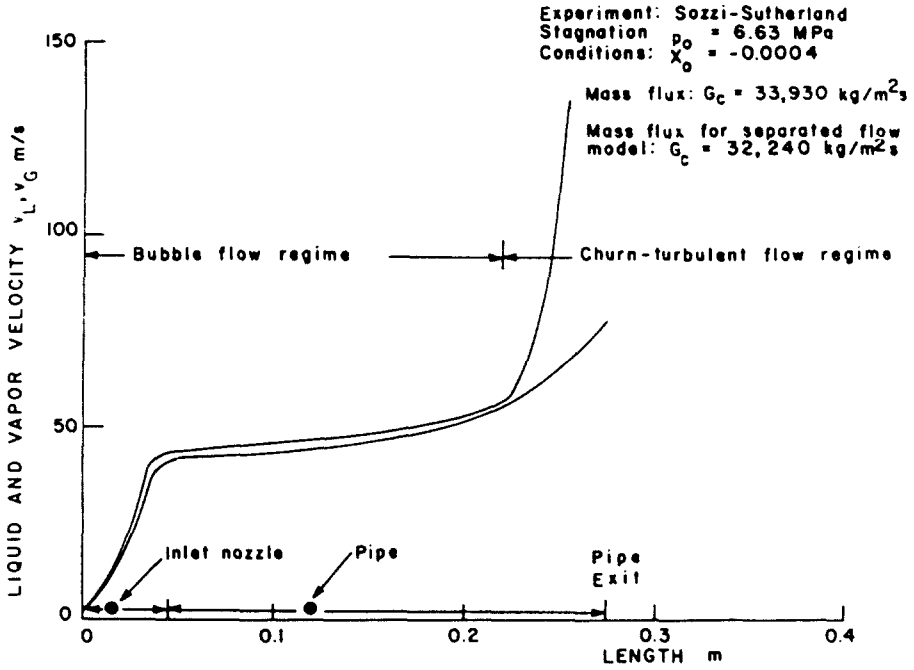

Figure 6. Liquid and vapor velocity vs length of test section calculated from separated flow model. (Experiment from Sozzi & Sutherland 1975).

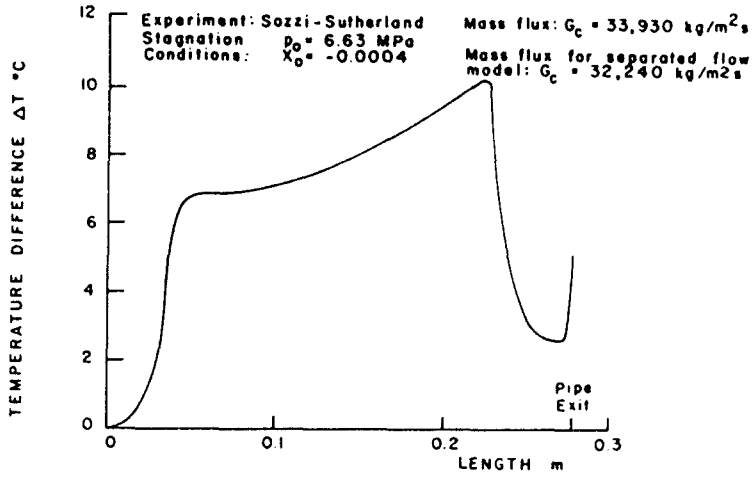

Figure 7. Temperature difference between liquid and vapor vs length of test selection calculated from separated flow model. (Experiment from Sozzi & Sutherland 1975).

—At the choking point, both thermal and hydrodynamic nonequilibrium become notable.

For very short pipes, nozzles and orifices the separated flow model predictions cannot be expected to be accurate since two-dimensional effects are presumably important. Figure 8 shows comparisons of this separated flow model with Edwards' (1968) theory, and experimental results by Fauske (1963). One should recall that Edwards introduced an additional empirical parameter to match the data for a short length of diameter ratio ($L/D < 5$).

Henry (1970) compared his experimental data with different theories described in Chapter 2. He found satisfactory agreement between his data and his empirical correlation (Figure 9). Further comparison with Zaloudek's (1964) data show that the Henry model is probably not applicable universally.

This separated flow model accounts for the different test geometries as well as different upstream conditions. It is capable of predicting the Henry as well as the Zaloudek data

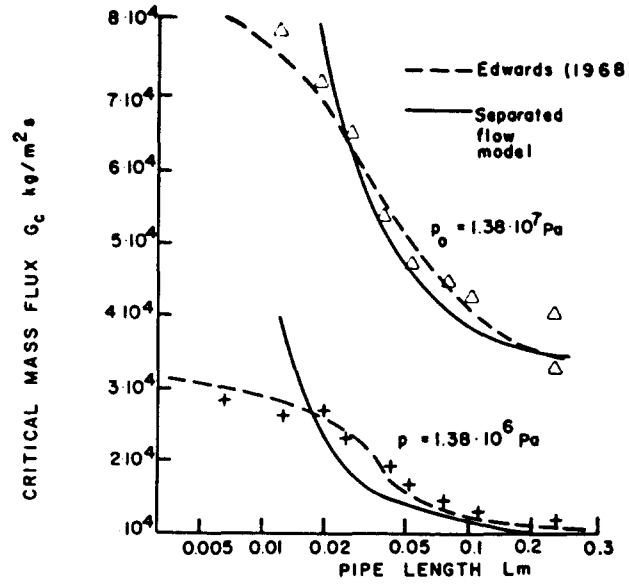

Figure 8. Comparison of separated flow model, Edwards' analysis and experiments for sharp-edged pipes (6.35 mm diameter). Stagnation conditions: saturated water.

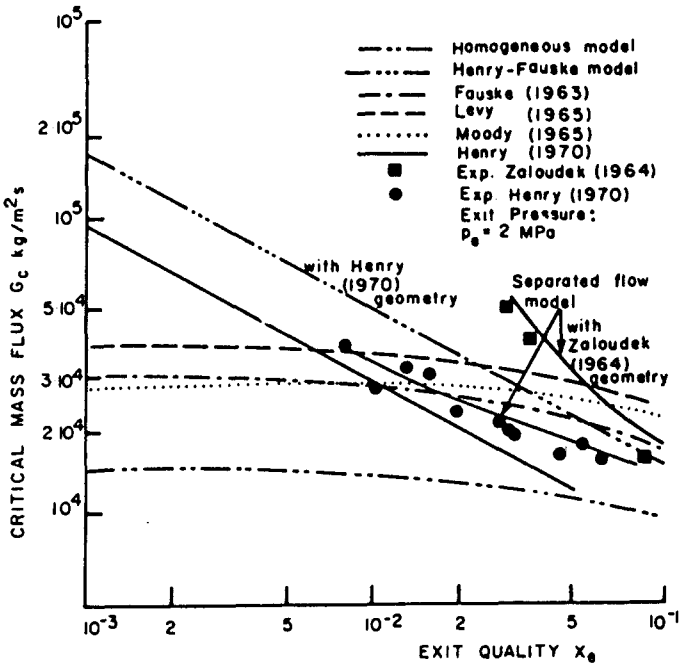

Figure 9. Comparison between analytical models and experimental data. (Henry 1970) and (Zaloudek 1964).

reasonably well (figure 9) Henry calculated the exit quality from the homogeneous energy equation. From this separated flow model the calculated exit quality is plotted vs the critical mass flux in figure 9. The exit pressure of all experiments shown in figure 9 is approximately 2 MPa. The calculations with this separated flow model result, in general, in a lower exit pressure.

In another experiment, Henry (1968) compared the measured critical mass flux with the homogeneous critical mass flux and plotted this ratio versus the homogeneous exit quality. He found a minimum in the critical mass flux ratio with increase in exit quality (figure 10). This minimum is probably due to a change in flow regime and it was particularly interesting to see if

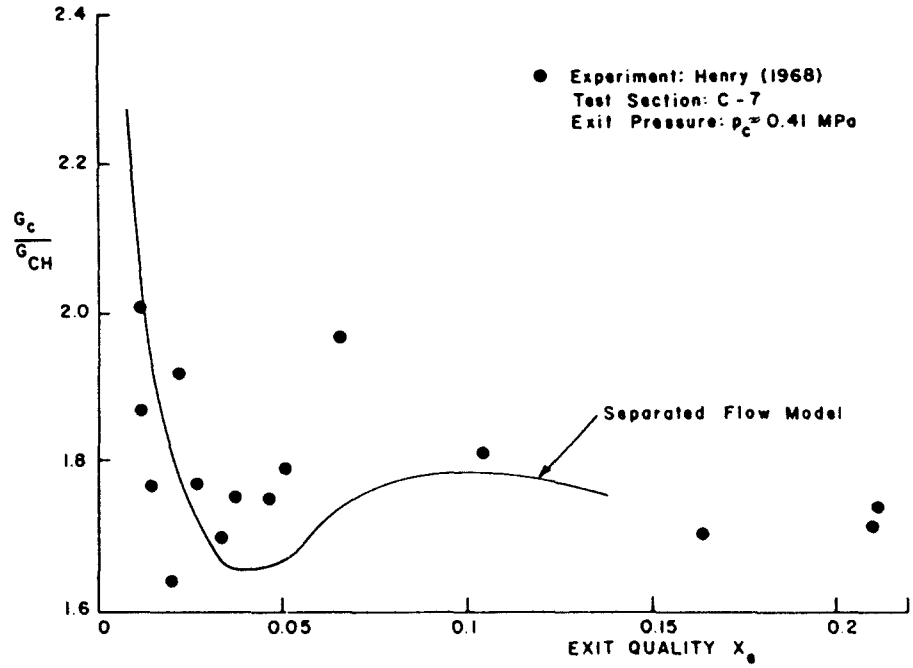

Figure 10. Ratio of critical mass flux to homogeneous critical mass flux vs exit quality. Comparison of data from Henry (1968) with the separated flow model.

this separated flow model would be capable of predicting this minimum as well. The results of the calculations with this model are indicated in figure 10. The agreement is very good and thus the original assumption of flow regime transition seems to be correct, as well as the void fraction, where this transition takes place.

In the above comparisons the actual exit quality calculated from the separated flow model was used rather than the homogeneous equilibrium quality. Further comparisons were performed with the experimental results of Sozzi & Sutherland (1975) in pipes of different lengths. In the experiments the pipe length after the inlet nozzle is varied.

The upstream conditions and the test geometry must be known to predict the critical mass flux with this separated flow model. Figures 11–14 show comparisons between the test data and the predictions.

The agreement is generally very good. Comparing results in figures 9–14 for different pipe lengths also indicates the decrease in mass flux with an increase in pipe length.

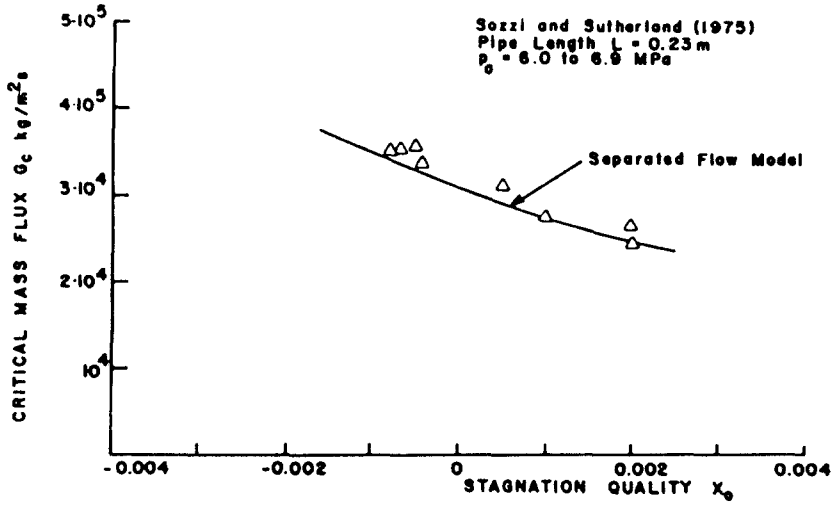

Figure 11. Critical mass flux vs stagnation quality. Comparison of Sozzi & Sutherland (1975) with the separated flow model. Pipe length L = 0.23 m.

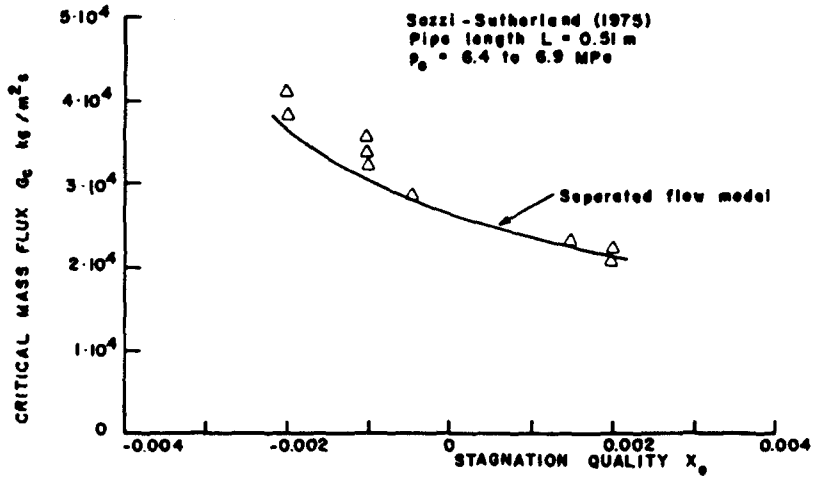

Figure 12. Critical mass flux vs stagnation quality. Comparison of Sozzi & Sutherland (1975) with the separated flow model. Pipe length $L = 0.51$ m.

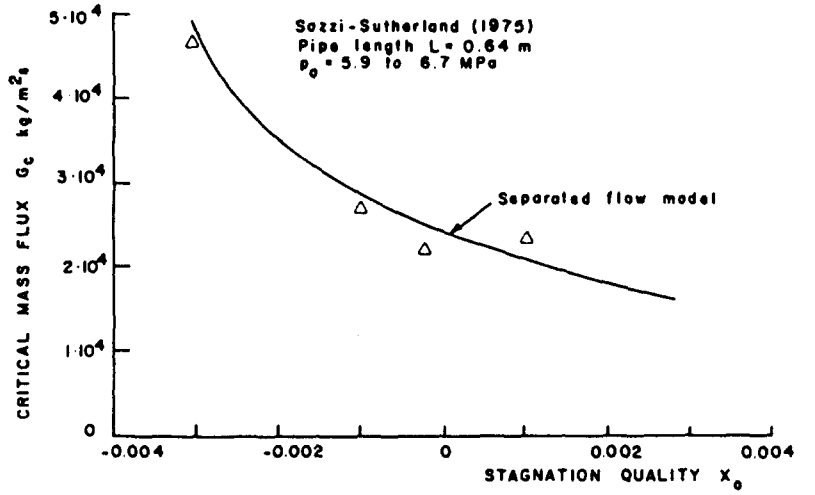

Figure 13. Critical mass flux vs stagnation quality. Comparison of Sozzi & Sutherland (1975) with the separated flow model. Pipe length $L = 0.64$ m.

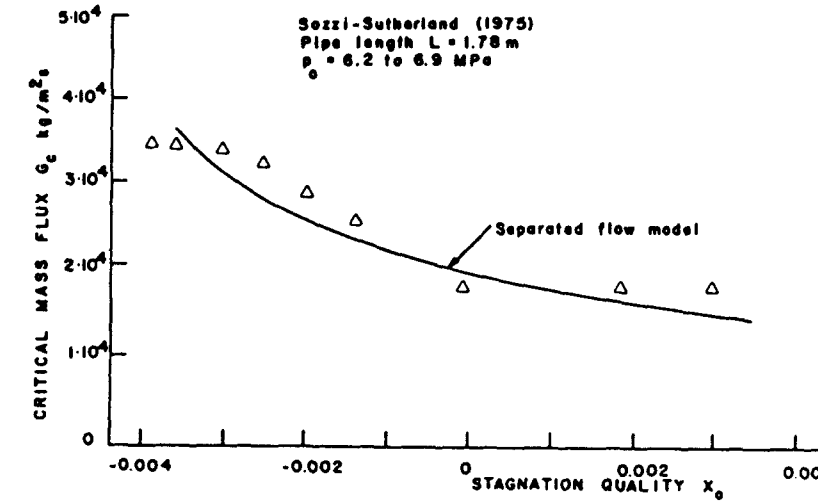

Figure 14. Critical mass flux vs stagnation quality. Comparison of Sozzi & Sutherland (1975) with the separated flow model. Pipe length $L = 1.78$ m.

CONCLUSIONS

A one dimensional separated flow model was developed to allow the calculation of critical two-phase flow. This model included hydrodynamic as well as thermal non-equilibrium. The relative velocities between the two-phases depend upon interfacial forces. The evaporation or condensation rate is restricted by heat transfer between these phases. Therefore, superheat is necessary to establish mass transfer.

Contingent upon the void fraction, different flow regimes are specified in this mode, like bubbly, churn-turbulent and annular. For the calculations, the upstream fluid conditions have to be known and the geometry of the test section.

In addition to the above, the initial bubble density has to be assumed. These bubbles are presumably present as dissolved gases acting as nucleation sites at the onset of flashing. The contribution of walls on the number of nucleation sites has been neglected. The initial bubble density of $N_i = 10^{11}\ m^{-3}$ for this model is similar to the assumption of other authors. If at the entrance to the flow conduit a two-phase mixture is already present, the bubble density can be quite different depending upon the past history of the flow.

Supplementally, the initial bubble diameter had to be described; this is equivalent to stating an initial void fraction. With this initial bubble diameter the superheat at onset of flashing can be evaluated. The superheat predicted on this basis seems to be in general agreement with measurements, Reocreux (1977).

Calculations of two-phase flow behavior in pipes and nozzles with this separated flow model show several interesting results. In the bubble flow regime the velocity difference between the two-phases is very small, therefore it is understandable that many investigators neglect it. But if we assume that the evaporation in expanding bubbly flow is limited by heat transfer, even small velocity differences become important for the overall heat transfer. During rapid depressurization in the bubbly flow regime the temperature difference between the two-phases increases substantially. The liquid superheats, indicating in that the bubbly flow regime thermal non-equilibrium is important. Unfortunately, these predictions of this separated flow model cannot be compared with experimental results, since measurements of temperature between the gas and liquid in rapidly accelerating flow are difficult to obtain.

The development of a separated flow model for other than bubbly or annular flow regimes is more difficult, since little is known about the interfacial transport processes. Thus certain empiricisms are necessary. The description of the churn-turbulent flow regime was deviced as a transition regime between the bubbly and the annular flow regime. At void fraction of $\alpha_b = 0.3$ transition from bubble to churn-turbulent flow regime is assumed. Coalescence of bubbles takes place, decreasing the interfacial area but increasing the relative velocity between vapor and liquid. From the detailed calculations we found that in churn-turbulent flow the temperature difference between the phases is not growing as rapidly as in bubble flow, in some cases it is even decreasing. We concluded from our calculations that hydrodynamic non-equilibrium is prevailing in the churn-turbulent flow regime. The transition from churn-turbulent to the annular flow regime is presumably taking place at a void fraction of $\alpha_a = 0.8$.

Comparison of critical mass flow rate predictions of this separated two-phase flow model with experimental results of several investigators shows generally good agreement. This indicates that the assumptions incorporated in this model are justified. The introduction of several flow regimes into this model is necessary to verify some of the experimental results.

Acknowledgement—This work was sponsored by the Electric Power Research Institute under Contract No. RP443-3. The Project Manager is Dr. K. H. Sun.

REFERENCES

ARDRON, K. H. & FURNESS, R. A. 1976 A Study of the critical flow models used in reactor blowdown analysis. *Nucl. Engng Design* **39**, 257–266.

ARDRON, K. H. 1978 A two-fluid model for critical vapor–liquid flow. *Int. J. Multiphase Flow* **4**, 323–337.

ARDRON, K. H. & ACKERMAN, M. C. 1978 Studies of the critical flow of subcooled water in a pipe, Central Electricity Generating Board, Berkeley, England, RD/B/N 4299.

BAILEY, J. F. 1951 Metastable flow of saturated water. *Trans. ASME* **73**, 1109–1116.

BOURÉ, J. A. 1974 Two-phase flows with application to nuclear reaction design problems. von Karman Institute for Fluid Dynamics, Lecture Series, Grenoble, France.

CRUVER, J. E. 1963 Metastable critical flow of steam–water mixtures. Ph.D. Thesis, University of Washington, Seattle.

EDWARDS, A. R. 1968. Conduction controlled flashing of a fluid, and the prediction of critical flow rates in a one-dimensional system. AHSB (S) R–147, UKAEA, AWRE, Foulness Islands, South End on Sea, Essex, England.

FAUSKE, H. K. 1963a Critical two-phase steam water flows. ANL-6633.

FAUSKE, H. K. 1963b Two-phase critical flow with application to liquid metal systems. ANL-6679.

HENRY, R. E. 1968 A study of one- and two-component, two-phase critical flows at low qualities. ANL-7430.

HENRY, R. E. 1970a An experimental study of low quality, steam–water critical flow at moderate pressures. ANL-7740.

HENRY, R. E. 1970b The two-phase critical discharge of initially saturated or subcooled liquid. *Nucl. Sci. Engng* **41**, 336–342.

HENRY, R. E. & FAUSKE, H. K. 1971 The two-phase critical flow of one-component mixtures in nozzles, orifices and tubes. *Trans. ASME J. Heat Transfer* **93**, 179–187.

ISBIN, H. S. 1980 Some observations on the status of two-phase critical flow models. *Int. J. Multiphase flows* **6**, 1–2, 131–138.

ISHII, M. 1975 *Thermo-Fluid Dynamics Theory in Two-Phase Flow*. Eyrolles, Paris.

JONES Jr., O. C. & SAHA, P. 1977 Non-equilibrium aspects of nuclear reactor safety", *Symposium on the Thermal and Hydraulic Aspects of Nuclear Reactor Safety*, Light Water Reactors, ASME, Vol. 1.

KUO, J. T., WALLIS, G. B. & RICHTER, H. J. 1979, Interphase momentum transfer in the flow of bubbles through nozzles. EPRI, NP–980.

MALNES, D. 1975. Critical two-phase flow based on non-equilibrium effects. ASME Meeting, Houston. *Non-Equilibrium Two-Phase Flows*, (Edited by R. T. LAHEY and G. B. WALLIS).

MUIR, J. F. & EICHHORN, R. 1967. Further studies of compressible flow of an air–water mixture through a vertical, two-dimensional converging–diverging nozzle. JSME Series, Int. Symposium, Tokyo, Japan.

PLESSET, M. S. & ZWICK, S. A. 1954. The growth of vapor bubbles in superheated liquids. *J. Appl. Phys.* **25**, 4.

REOCREUX, M. L. 1976 Experimental study of steam–water choked flow. Specialists Meeting on Transient Two-Phase Flow, Toronto.

REOCREUX, M. L. 1977 Contribution to the study of the critical flow rates in two-phase water vapor flow. NUREG–TR–0002, 1–3.

RICHTER, H. J. & MINAS, S. E. 1979 Separated flow model for critical two-phase flow. ASME Meeting, San Diego, Non-Equilibrium Interfacial Transport Processes.

RICHTER, H. J. 1981 Separated two-phase flow: Application to critical two-phase flow. EPRI, NP–1800.

RIVARD, W. C. & TRAVIS, J. R. 1980 A non-equilibrium vapor production model for critical flow. *Nucl. Sci. Engng* **74**, 40–48.

ROHATGI, U. S. & RESHOTKO, E. 1975 Non-equilibrium two-phase flow through quasi one-dimensional chennels. Dept. Fluid, Thermal and Aerospace Sciences, Castle Western Reserve University, FTAS/TR–75–115.

ROWE, P. N. & HENWOOD, C. A. 1961 Drag Forces in a hydraulic model of a fluidized bed, part I. *Trans. Inst. Chem. Engng* **39**, 43–54.

SAHA, P. 1978. A review of two-phase steam–water critical flow models with emphasis on thermal non-equilibrium. NUREG/CR[0417, BNL–NUREG–50907.

SCHROK, V. E., STARKMAN, E. S. & BROWN, R. A. 1977 Flashing flow of initially subcooled water in covergent–divergent nozzles. *trans. ASME, J. Heat Transfer* **99**, 263–268.

SIMON, U. 1972. Blowdown flow rates of initially saturated water. ANS Salt Lake City Meeting, 172–175.

SOZZI, G. L. & SUTHERLAND, W. A. 1975a. Critical flow for saturated and subcooled water at high pressure. ASME Meeting. Houston, Non-Equilibrium Two-Phase Flows (Edited by L. T. LAHEY and G. B. WALLIS).

SOZZI, G. L. & WUTHERLAND, W. A. 1975b Critical flow of saturated and subcooled water at high pressure. GE Report NEDO–13418.

VANCE, W. H. 1962 A study of slip ratio for the flow of steam–water mixtures at high void fractions. Ph.D. Thesis, University of Washington, Seattle.

WALLIS, G. B. 1969 *One-Dimensional Two-Phase Flow*. McGraw-Hill, New York.

WALLIS, G. B. 1980. Critical Two-phsse flow. *Int. J. Multiphase Flow* **6**, 97–112.

WOLFERT, K. 1976. The simulation of blowdown processes with consideration of thermodynamic non-equilibrium phenomena. Specialists Meeting on transients Two-Phase Flow, Toronto.

ZALUDEK, F. R. 1964 Steam–water critical flow from high pressure systems. GE Report HW 80535.

ZALOUDEK, F. R. 1965 The low pressure critical discharge of steam–water mixtures from pipe elbows and tees. BNWL–34 UC–38.

ZIVI S. M. 1964. Estimation of steady-state steam void fraction by means of the principle of minimum entropy production. *J. Heat Transfer* 247–252.